Chapter 2

Four-Quadrant Control of Switched Reluctance Machine

Sandeep Narla

Additional information is available at the end of the chapter

http://dx.doi.org/10.5772/intechopen.69228

Abstract

This chapter illustrates modeling techniques and software simulation of the switched reluctance machine (SRM) machine models with controllers for efficient operation. The first model is based on torque and flux data generated through finite element analysis (FEA) and the second model is geometry-based machine model, which are used to develop the operation logic for four-quadrant control of an SRM. The results obtained from these models were used to develop a control strategy to adapt turn-on and turn-off (commutation) angles efficiently. Two digital controllers, namely the phase current controller for regulating current with a hysteresis band and the PI (proportional-integral) speed controller for regulating the speed, are developed to deliver the desired output torque. The controller is based on a negative feedback closed-loop control system.

Keywords: SRM, four-quadrant, motoring, generating, FEA, modeling, simulation

1. Introduction

Earlier chapters may have described the fundamental principles of the SRM such as its stator, rotor configuration, construction, and basic operation. The shape of the inductance profile of a switched reluctance machine (SRM) along the air-gap between stator and rotor poles depends on the resistance along the gap and pole-widths of stator and rotor as shown in **Figure 1**. The control algorithm is developed based on this inductance profile with respect to rotor position. Motoring can be achieved between unaligned and aligned pole positions because of the positive slope of inductance. Similarly, along the negative slope from aligned to unaligned pole positions, generating torque can be produced [1].

During motoring operation, the machine produces positive torque between unaligned and the next aligned position in forward or reverse directions. In generation, the inductance will be

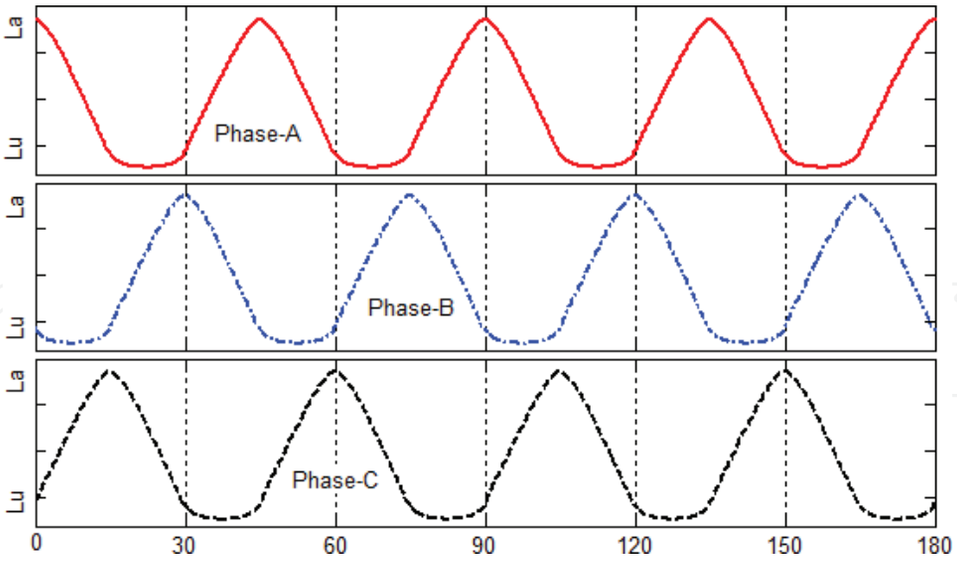

Figure 1. Phase inductance profile of a 12/8 pole SRM with respect to rotor position (in mechanical degrees).

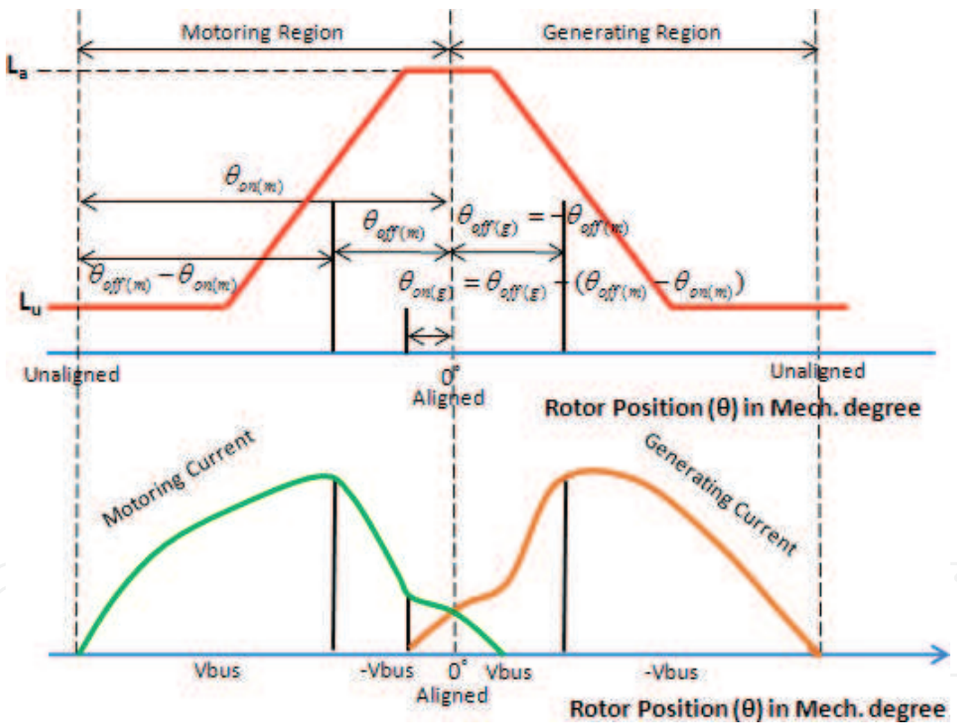

Figure 2. Motoring and generating current waveforms describing the phase inductance principle of SRMs.

decreasing in the direction of rotation resulting in negative torque. The current flow in the phase winding is always unidirectional; however, the current profiles for the motoring and generating modes are exactly the mirror image of each other along the aligned pole position for the same speed and symmetrical turn-on and turn-off angles as shown in **Figure 2**.

http://dx.doi.org/10.5772/intechopen.69228

2. Classic converter topology

Since the torque developed in an SRM is independent of the direction of current flow, unipolar converters are sufficient to serve as the power converter circuit for the SRM. The most flexible and versatile four-quadrant SRM topology is the classic bridge converter, which has two transistors and two freewheeling diodes per phase as shown in **Figure 3**. The transistor switches are turned on and off in each phase based on the controller output for torque and speed control of the SRM.

There are three modes of converter operation in each phase: magnetization, freewheeling, and demagnetization.

1. Magnetization period for motoring is when both the switches are turned on and the energy is transferred from the source to the motor phase winding as shown in **Figure 4(a)**. For generation, the phase winding of the motor is excited initially to generate higher back-emf than the DC-link voltage ($+V_{dc}$) with the machine driven by a prime mover. The generated energy is delivered to the electrical side achieving generation.

2. Freewheeling, for motoring operation at lower speeds, is accomplished by keeping one of the switches on and switching the other switch as shown in **Figure 4(b)**. With only one switch on, the motor phase gets slowly demagnetized through the respective antiparallel freewheeling diode. For generating operation, one of the switches is turned off, whereas the other switch is turned on and off. With only one switch on, the motor phase gets slowly magnetized through the respective antiparallel freewheeling diode.

3. Demagnetization is achieved by applying a negative DC-link voltage to the phase winding with the two switches turned off as shown in **Figure 4(c)**, helps in fast decay of current flowing through both the diodes.

The chopping operation involves switching of the transistors connected to the phase winding accordingly for current regulation depending on the motoring or generating operation. The possible phase voltages in this Pulse Width Modulation (PWM) operation would be $+V_{dc}$ (for magnetization), 0 V (freewheeling), and $-V_{dc}$ (for demagnetization). The phase current control is set by three levels, which include the reference current value "I_{ref}" and the upper and lower hysteresis band limits. The hysteresis band value is chosen based on the peak current value of the machine. The chopping operation is implemented for torque control below the based speed.

The single-pulse mode of operation is possible when the machine is operated at high speeds. The possible phase voltages in this operation would be $+V_{dc}$ (for magnetization) and $-V_{dc}$ (for demagnetization). The current regulation is not possible in this operation because in motoring there may not be sufficient time to reach the desired current level at high speeds or in generating, when demagnetization occurs, there is no control over the diodes. The main advantage of this converter is its ability for independent control of each phase, which is particularly important when phase overlap is desired. It is more suitable for high-voltage, high-power drives.

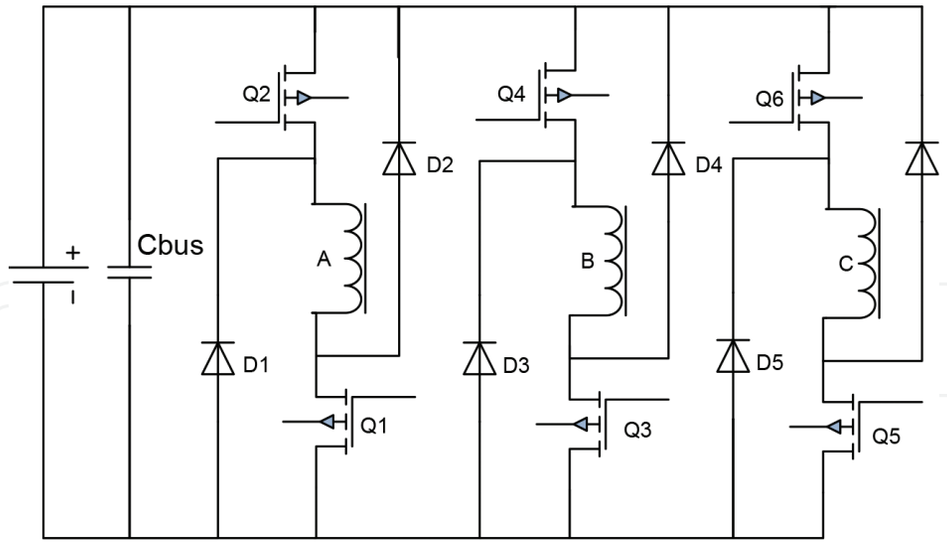

Figure 3. Four-quadrant classic converter for a three-phase SRM.

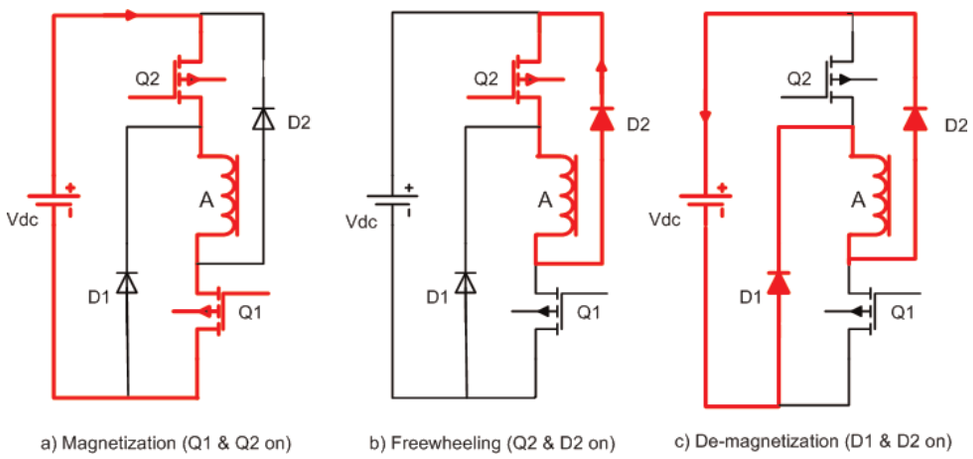

Figure 4. Converter switching operation for motoring of phase A winding.

3. Controller strategy

The effective performance characteristics from an SRM drive system can be obtained by proper positioning of the phase excitation pulses relative to the rotor position. The commutation angles (turn-on angle "θ_{on}," turn-off angle "θ_{off}"), total conduction period, and the magnitude of the phase current "I_{ref}" determine the average torque, torque ripple, and other performance parameters. The complexity of finding the control parameters depends on the chosen control method for a particular application. At low speeds, the current rises almost instantaneously after turn on because of the negligible back-emf and the current must be limited by either controlling the average voltage or by regulating the current level. As the speed increases, the back-emf increases and opposes the applied DC-link voltage. Phase advancing is necessary to establish the phase current at the onset of rotor and stator pole overlap region. Voltage PWM is used to force maximum current into the machine to maintain the desired torque level.

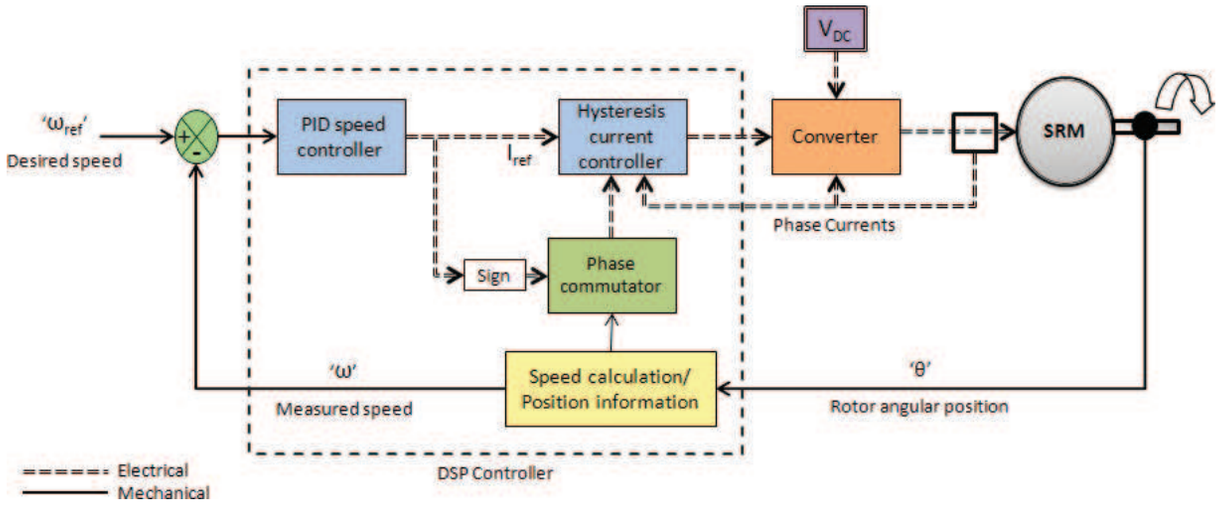

Figure 5. Closed-loop speed and current control block diagram of a SRM.

The block diagram for the general closed-loop speed and current control of the SRM is shown in **Figure 5**. In speed control applications, an outer speed loop is added to the faster inner current loop. The inner loop creates desired currents in the stator windings necessary to achieve the desired speed specified by the outer loop. The inner current loop is implemented by current regulation, which consists of the current controller, the power converter, the SRM stator windings and the current sensing devices for feedback control. For current control, a simple hysteresis controller is illustrated here for simplicity and PI controller for outer speed control.

4. Modeling of SRM in finite element analysis

Flux 2D is a finite element analysis software by Magsoft Corporation [2] that allows the user to determine the various characteristic parameters of a machine based on the mechanical dimensions, material properties, and operating conditions of the machine [10]. The overall cross-section of the machine is divided into many sections, such as shaft, rotor, air-gap, stator, and so on, and individual properties are defined. At the intersections of each section and on the surface, the desired machine parameters of the SRM are calculated by virtually running the machine at a constant speed in small position steps. The finite element analysis gives the flux-linkage and torque characteristics of the SRM with respect to rotor position and current level. These characteristics are used to build the SRM model in the form of look-up table. The developed look-up table model is used in the simulation of the machine model.

An Finite Element Analysis (FEA) package requires detailed input data as shown in **Table 1** for design and the results need skilled interpretation. The SRM operates in a series of strokes with "switched mode" excitations having no steady-state reference where all its state variables are constant. The initial sizing of the geometry, static and magneto-dynamic FEA and system-level simulations should be considered simultaneously for the SRM design to meet the design requirements [3]. Other design objectives can be to optimize the torque density, power density, efficiency and to minimize torque ripple.

Parameters	Value	Units
Shaft radius	0.6	Inches
Radius to rotor yoke	1.2025	Inches
Radius to air gap	1.6325	Inches
Radius to stator yoke	2.233	Inches
Outer radius	2.7435	Inches
Air-gap	0.015	Inches
Number of phases	3	–
Number of stator poles	12	–
Number of rotor poles	8	–
Number of repetitions	2	–
Periodicity	90	Degrees
Rotor pole width	15	Degrees
Stator pole separation	30	Degrees
Magnetic saturation	1.8	Tesla
Magnetic permeability	4pi × e-7	Henry/meter
Relative permeability	3300	–
Fill factor	0.453	–
Stacking factor	0.9	–
Length of stack	1.846	Inches
Phase resistance	2.1	Ohms
No. of turns/pole	175	–
No. of coils in series	4	–
No. of coils in parallel	1	–
Max. current in coil	5.5	Amperes
Power delivered	660	Watts
Operating speed	264	Radians/sec

Table 1. Dimensions, configuration parameters, and ratings of an example 3-ph, 12/8 SRM.

Modeling of SRM in Flux 2D involves eight steps: (a) geometry construction, (b) sectional design, (c) surface meshing, (d) stator and rotor material, (e) stator coil excitation circuit, (f) rotor physics definition, (g) solving for machine parameters, and (h) analysis of results [4].

5. Simulation of the SRM FEA model in Mat-lab

Look-up tables are developed for the machine model from the flux-linkage and torque characteristics obtained from FEA. The flowchart showing the SRM simulation with FEA look-up

http://dx.doi.org/10.5772/intechopen.69228

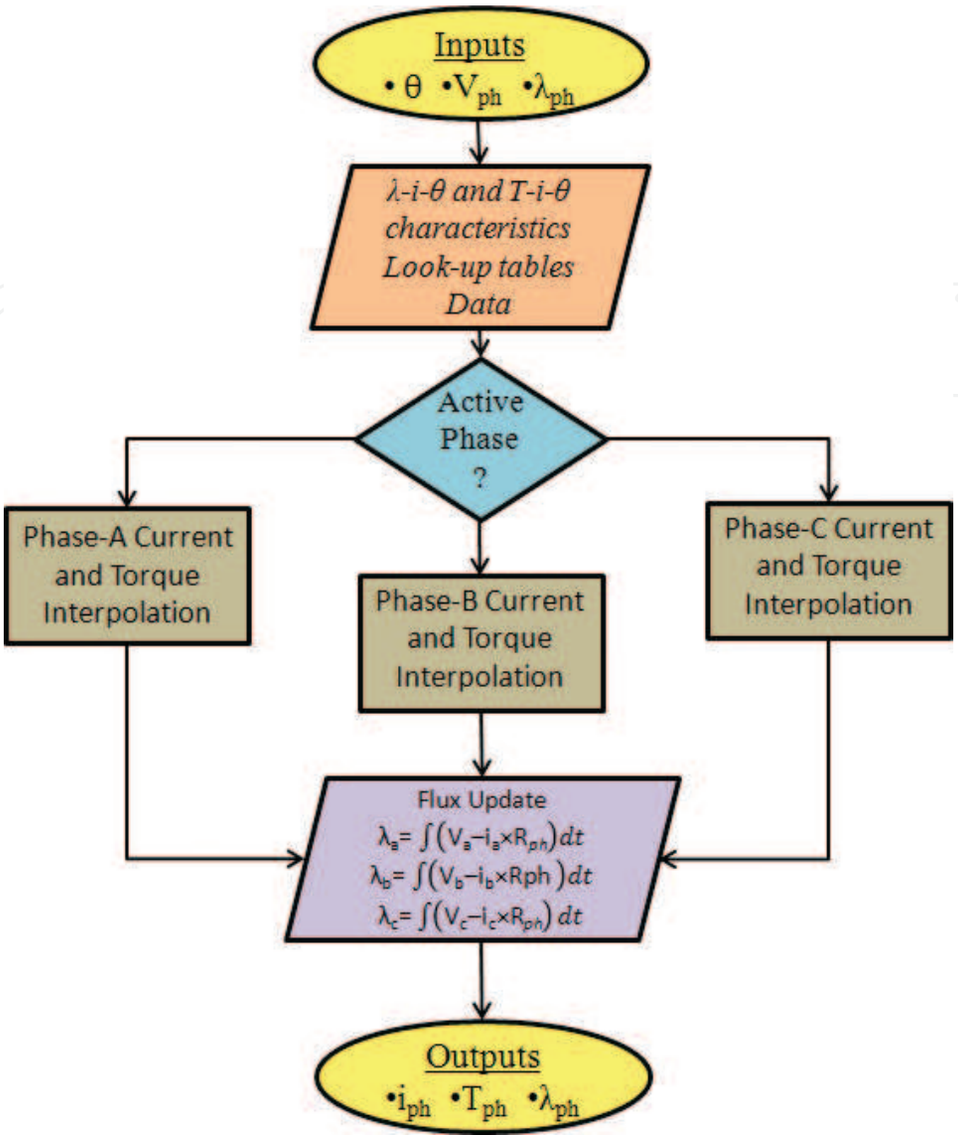

Figure 6. Flowchart showing the SRM simulation with FEA look-up table-based model.

table-based model is shown in **Figure 6**. The control logic for this simulation is similar to the geometry-based machine model described below. The table for flux-linkage characteristics consists of flux values at different current levels and rotor positions as shown in **Figure 7**. The table for torque characteristics consists of phase torque values for different current levels and rotor positions as shown in **Figure 8**. Depending on the mode of operation (motoring or generating), the respective rotor positions are considered appropriately.

5.1. Phase current interpolation

In the flux-linkage table, the columns represent the phase current (in amperes) and the rows represent the rotor position (in degrees). The flux-linkage values at different rotor positions are represented as rows between unaligned and aligned positions. Now depending on the rotor position and the flux-linkage values, the two adjacent current columns are known. Finally, the

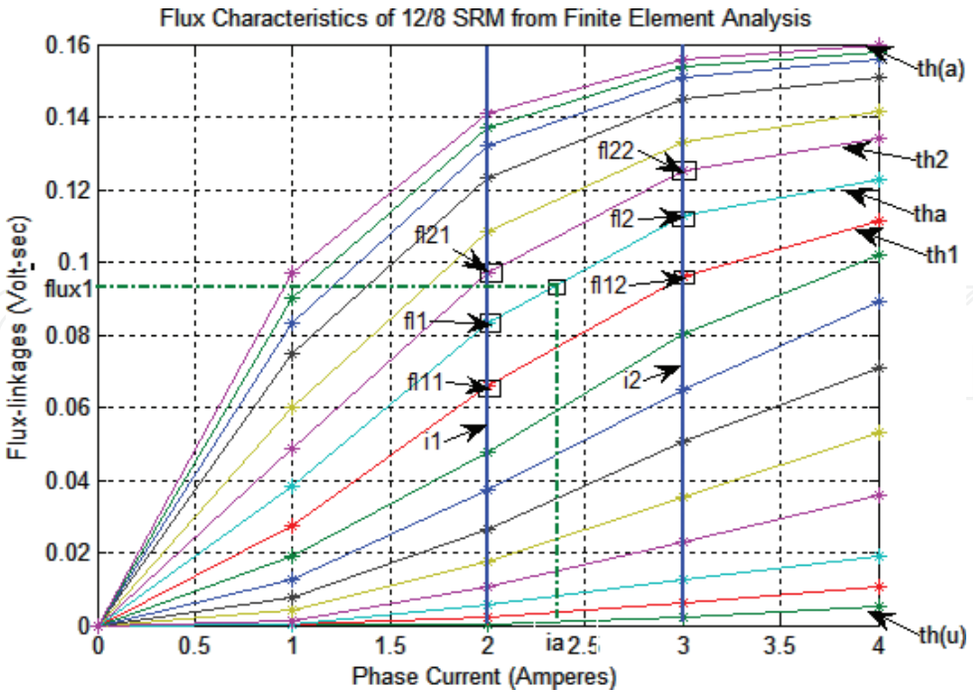

Figure 7. Flux-linkage characteristics obtained from Flux2D finite element analysis.

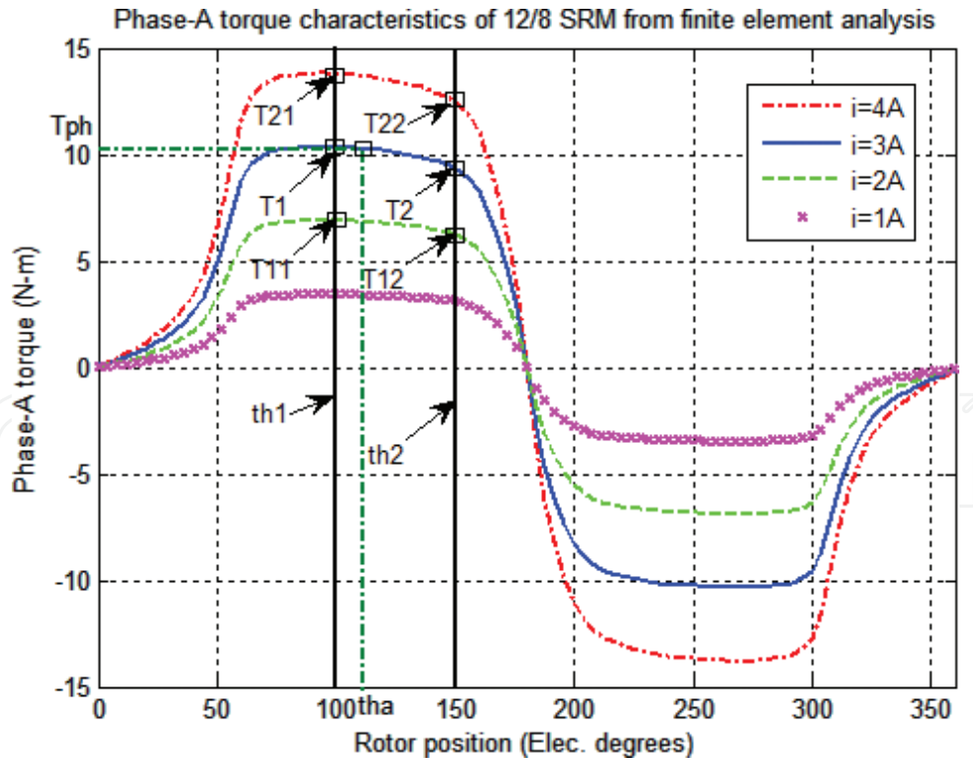

Figure 8. Torque characteristics obtained from Flux2D finite element analysis.

phase current is interpolated from this data as shown in Eqs. (1)–(8). The interpolation algorithm is described below.

A set of four fluxes is obtained first from available data in flux-linkage table. These are

$$fl_{11} = flux(row_1,\ col_1) \tag{1}$$

$$fl_{12} = flux(row_1,\ col_2) \tag{2}$$

$$fl_{21} = flux(row_2,\ col_1) \tag{3}$$

$$fl_{22} = flux(row_2,\ col_2) \tag{4}$$

The interpolated fluxes fl_1, fl_2 are obtained from fl_{11}, fl_{12}, fl_{21}, fl_{22}, respectively, using the equation:

$$fl_1 = (fl_{21} - fl_{11}) \times (\ th_1 - th_1)/(\ th_2 - th_1)\ + fl_{11} \tag{5}$$

$$fl_2 = (fl_{22} - fl_{12}) \times (\ th_1 - th_1)/(\ th_2 - th_1) + fl_{12} \tag{6}$$

Here, th_a is in mechanical degrees.

The final phase current at fixed "th_a" is calculated as:

$$i_{ph} = (i_2 - i_1) \times (phase\_flux - fl_1)/(fl_2 - fl_1) + i_1 \tag{7}$$

After determining the appropriate phase current value, the rate of change of flux-linkage is computed based on the equation below. By integrating the above equation, the instantaneous phase flux-linkages can be obtained.

$$d\lambda_{ph}/dt = V_{ph} - (i_{ph} \times xR_{ph}) \tag{8}$$

5.2. Phase torque interpolation

Similar to phase current, the phase torque is also interpolated using the same procedure [12]. The interpolation equations with reference to the **Figure 8** below are given in Eqs. (9)–(11).

$$T_1 = (T_{21} - T_{11}) \times (th_a - th_1)/(th_2 - th_1) + T_{11} \tag{9}$$

$$T_2 = (T_{22} - T_{12}) \times (th_a - th_1)/(th_2 - th_1) + T_{12} \tag{10}$$

Here, th_a is in mechanical degrees.

The final phase torque at fixed "th_a" is calculated as:

$$T_{ph} = (T_2 - T_1) \times (i_{ph} - i_1)/(i_2 - i_1) + T_1 \tag{11}$$

6. Modeling of SRM in Mat-lab

The SRM is always operated in the magnetically saturated mode to maximize the energy transfer. Knowledge of the magnetic flux linked by a phase is essential to develop a sophisticated SRM controller. The inherent magnetic non-linearity of the SRM must be taken into account by accurate modeling of the machine characteristics [5]. The high degree of non-linearity makes it [9] impossible to model the flux-linkage or phase inductance by an SRM phase accurately. The phase inductance and flux-linkage vary with rotor position due to stator and rotor saliencies and also vary with the instantaneous phase current because of magnetic saturation.

The analytical model developed by A. Radun is derived from the machine geometry and material magnetic property. The model uses an analytical solution for the flux linked and static torque produced by one SRM phase. Separate analytical models for the flux linked by a phase when its stator and rotor poles do overlap [6] and do not overlap [6] are combined to provide a complete model of a given SRM phase. When the poles overlap, saturation must be included, especially in the pole tips, whereas a linear representation can be used for the unsaturated regions. The flux linked by the SRM phase is determined from the sum of the main flux and the fringing flux that is linked to the phase. The analytical model could be used to calculate motor parameters.

The geometry-based machine model allows extensive computer simulation studies during the machine and drives design stage. The general form of a geometry-based analytical expression for flux-linkage used can be shown as [6]:

$$\lambda(i,\theta) = A_m(\theta,\xi) + A_f(\theta,\xi) - B_m(\theta,\xi) \times sqrt\left(C_m(\xi) + D_m(\theta,\xi) + E_m\left(i^2,\xi\right)\right) - B_f(\theta,\xi) \times sqrt\left(C_f(\xi) + D_f(\theta,\xi) + E_f(i^2,\xi)\right) \tag{12}$$

Where, A, B, C, D, and E are dependent constants. "ξ" stands for geometry and magnetic

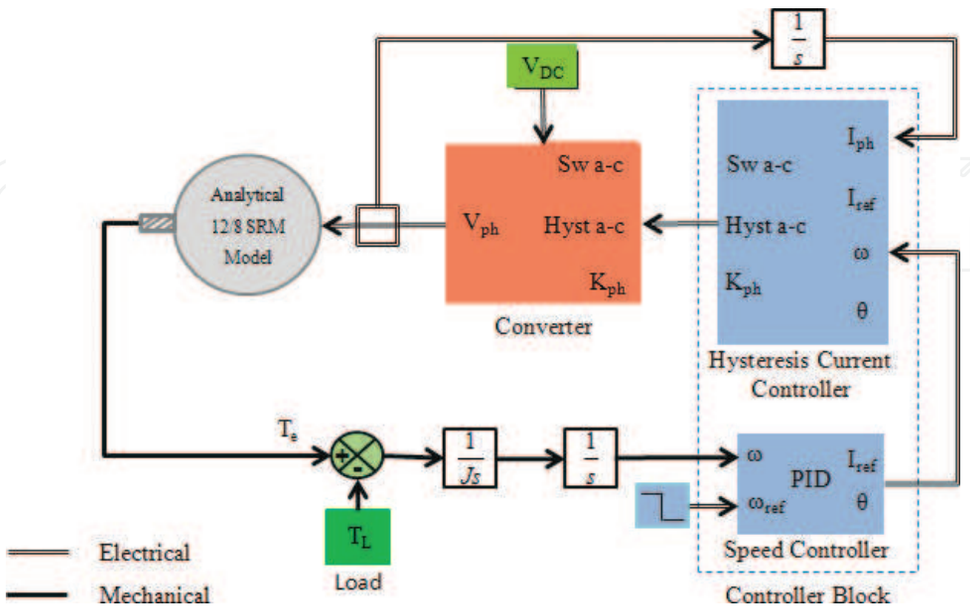

Figure 9. Simulation block diagram of analytical SRM model.

properties and "θ" stands for rotor position. Subscripts "m" and "f" are for main and fringing components of the flux-linkage, respectively. This approach is important for modeling of the magnetic structure of the motor for the purposes of controller design and dynamic performance prediction.

The above model described is used in the mat-lab simulation [7]. The block diagram of the simulation is shown in **Figure 9**. The modules for the simulation are the machine model, the speed and current controllers, the power converter, and the load model. The inputs to the machine model are the phase voltages, and the outputs are the phase currents, rotor position, and electromagnetic torque. In the machine model, the current derivatives *di*/*dt* are calculated based on the machine parameters, applied phase voltages, and the previous step phase currents and position information. The equations to calculate the phase torque, phase inductance, back-emf and phase currents have been derived from the machine model. The fundamental inputs used for this simulation are the geometric parameters and operating conditions of the machine.

7. Simulation of the SRM analytical model in Mat-lab

The controller generates the turn on, turn off, and phase current command based on a control algorithm and rotor position feedback information [11]. The sequence of phase turn-on and turn-off logic for each phase is simplified by wrapping the angles for once rotor pole period, i.e., −22.5 to 22.5° based on the 12/8 pole SRM configuration shown in **Figure 10**. Since the machine has 12 stator and 8 rotor poles, the pole arc of each rotor pole is 45°; therefore, the position is periodic within −22.5 to 22.5° or 22.5 to −22.5° depending on the direction of rotation (forward or reverse directions, respectively). Similarly, the position wrapping for phase *B* and *C* are shifted by 30 and 60° (mechanical) respectively [8].

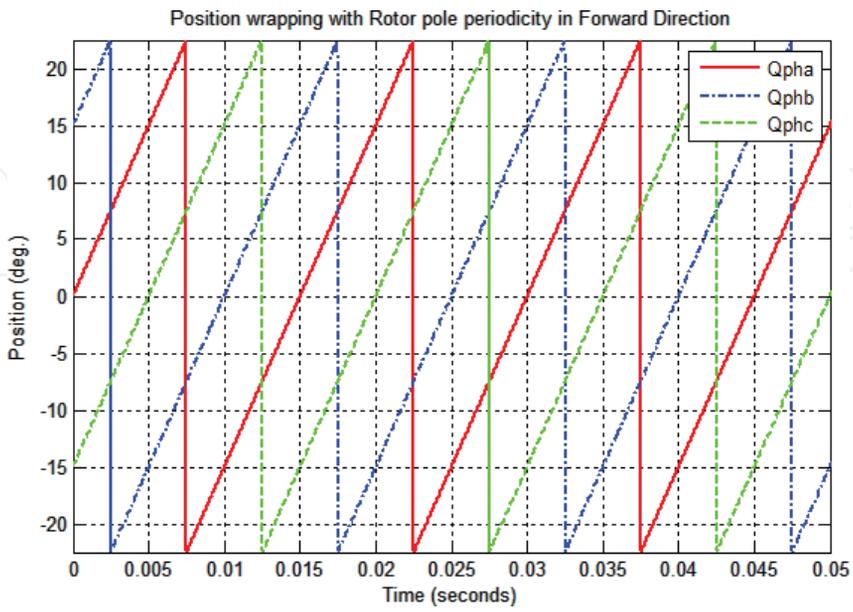

Figure 10. Position wrapping of each phase with rotor pole arc period.

7.1. Motoring operation of the SRM

The best turn-on and turn-off angles are tuned for proper current and speed control based on the inductance profile of the machine [13]. The various operations involved in modeling the closed-loop control of the SRM for motoring are active phase determination, phase switching, hysteresis current chopping, and PI speed control.

a. **Active phase determination:** The active phase to be turned on for power processing is based on the rotor position. Phase A aligned position is used as the reference (initialized to 0°); therefore, phase C will be starting phase for motoring operation if going in forward direction of motion or phase B if going in reverse direction. When the phase is operating in its increasing inductance region and within the conduction period, it is said to be active. The turn-on and turn-off angles may change, and the period of phase operation may also vary depending on the torque demand and operating speed. The nominal phase conduction period is the stroke angle, which is 15° for a 12/8 SRM.

b. **Phase commutation:** In order to achieve precise control of phase current at various machine operating speeds, each active phase has to be operated between the optimum turn-on and turn-off angle positions. When the phase operation starts, the winding is excited until the current command is reached and then demagnetized when the phase operation is turned off. Chopping can also be implemented for torque control.

c. **Current chopping:** Once the phase is excited with both switches turned on $+V_{\mathrm{dc}}$ is applied, the phase current will increase as the phase voltage dominates over the back-emf resulting in positive di/dt as described by Eq. (13):

$$di/dt = (V_{ph} - back\_emf - i \times R_{ph})/L_{inc}(\theta) \tag{13}$$

When the current reaches the upper band $[I_{\mathrm{ref}} + band/2]$, one of the switches is turned off, whereas the other switch is kept on for the phase current to decrease by freewheeling within the phase winding because of negative di/dt. When the current reaches the lower band $[I_{\mathrm{ref}} - band/2]$ due to 0 V, both the switches are turned on to increase the phase current. Both the switches are turned off when the phase has to commute upon approaching the turn-off angle so that the phase current decays to zero quickly as shown in **Figure 12**. During motoring operation, the phase voltage applied across the phase winding by switching of transistors is shown in **Figure 11**. This procedure is repeated for next in-coming phases.

The machine rotor speed "ω_{m}" and position "θ" is computed with the known moment of inertia "J" the total electromagnetic torque "T_{e}" developed by the machine, and the opposing load torque "T_{L}" using the equation;

$$J \times d\omega/dt = T_e - T_L \tag{14}$$

d. **PI speed controller:** A PI controller is used for speed control of the SRM for simplicity. The advantage with this controller is that the speed of the machine can be controlled with fast

transient without overshoots and good stead state response. The PI speed control loop is in the outer loop generating the desired phase current command based on the speed as shown in closed-loop block diagram **Figure 5**. Here, the desired current "I_{ref}" is not fixed, but changes based on the error between desired speed "ω_{ref}" and actual machine speed "ω". The PI control parameters are tuned in the simulation **Figure 12**.

7.2. Generating operation of the SRM

Here, the SRM is mechanically coupled and driven by the prime mover at a constant speed. The various operations involved in modeling the braking operation of the SRM are active phase determination, phase commutation, and hysteresis current chopping [14].

a. Active phase determination: Generation is achieved during decreasing inductance region $-dL/d\theta$ from aligned to unaligned positions. The conduction angle in this region is chosen based on the control algorithm for desired braking operation. The same turn-on and turn-off angles are used for other phases with phase angle shifting. The turn-on and turn-off angles may change depending on the speed and generation current command.

b. **Phase commutation:** The phase operation in generation is quite different from motoring operation. When the phase switching is turned on, the winding is initially excited for some period and then generation is achieved with the excitation turned off. When the excitation is off, the phase winding is demagnetized through the diodes in order to capture the generated energy. Chopping mode with hysteresis current control can also be used for regeneration in the lower speed range.

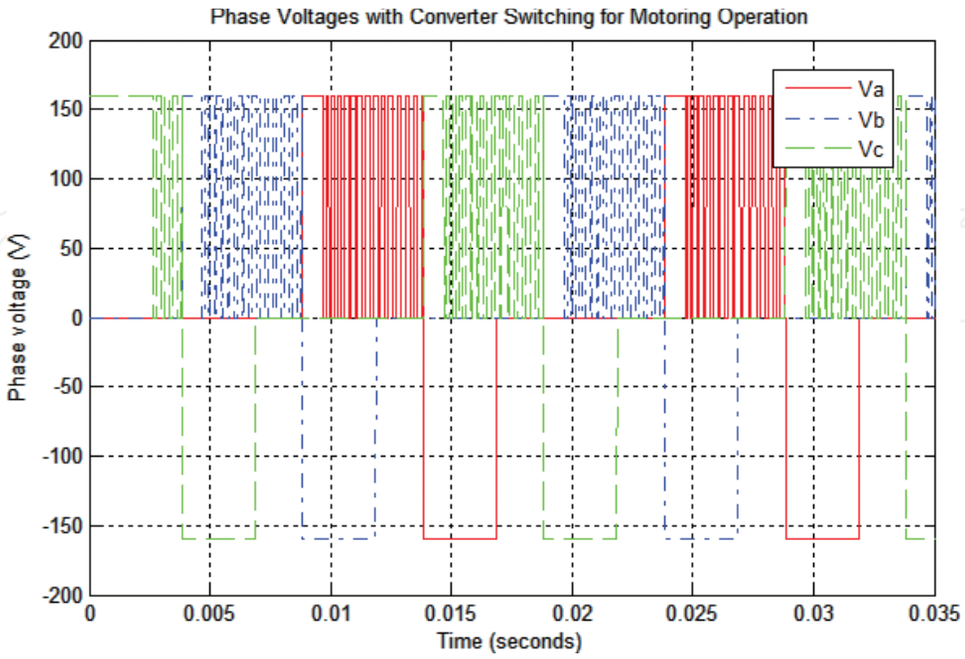

Figure 11. Phase voltage switching during motoring operation at fixed speed.

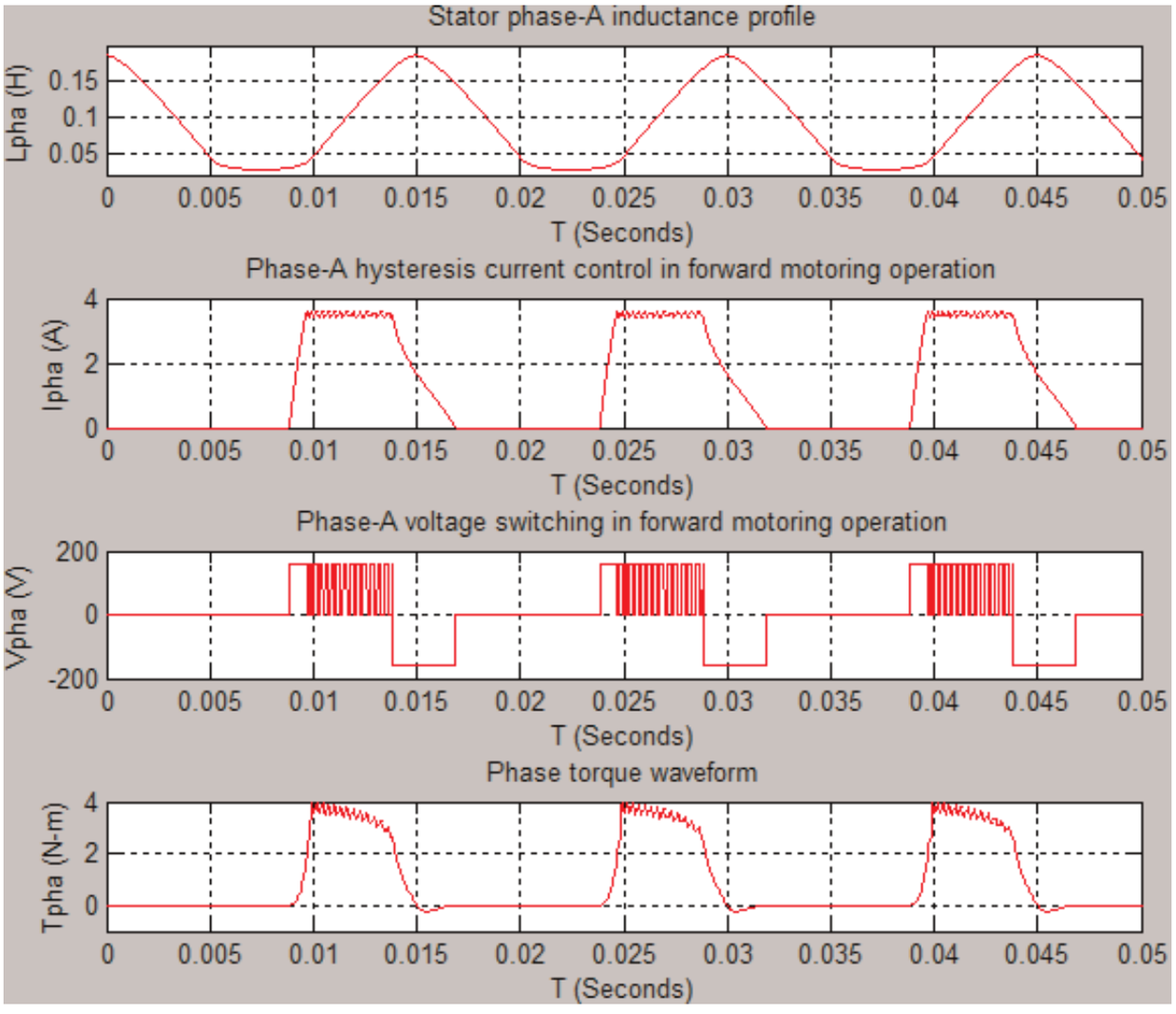

Figure 12. Forward motoring operation of phase A with hysteresis current control.

c. Current chopping: The phase current control is implemented same as in motoring, but the freewheeling of phase currents is achieved differently. The back-emf produced during the generation is negative; therefore, when the voltage across phase winding is 0 V, the rate of current change is positive resulting in magnetization. Similarly, with the phase voltage $-V_{\mathrm{dc}}$ the rate of current change is negative resulting in current decay based on Eq. [13].

The phase winding is initially excited for some period by applying $+V_{dc}$ across the phase. When the phase excitation is turned off, the phase current will continue to increase even after the excitation period is finished and the current regulation follows until the phase operation is commuted. During current regulation, when the current reaches the upper band $[I_{\mathrm{ref}} + band/2]$, both the switches are turned off $(-V_{\mathrm{dc}})$ and when the current reaches the lower band $[I_{\mathrm{ref}} - band/2]$, one of the switches is turned on (0 V) to freewheel the current within the phase winding. When the phase has to commute, both the switches are turned off $(-V_{\mathrm{dc}})$ to let the phase current decay to zero soon and then set to 0 V, when the current reaches zero as shown in **Figure 13**.

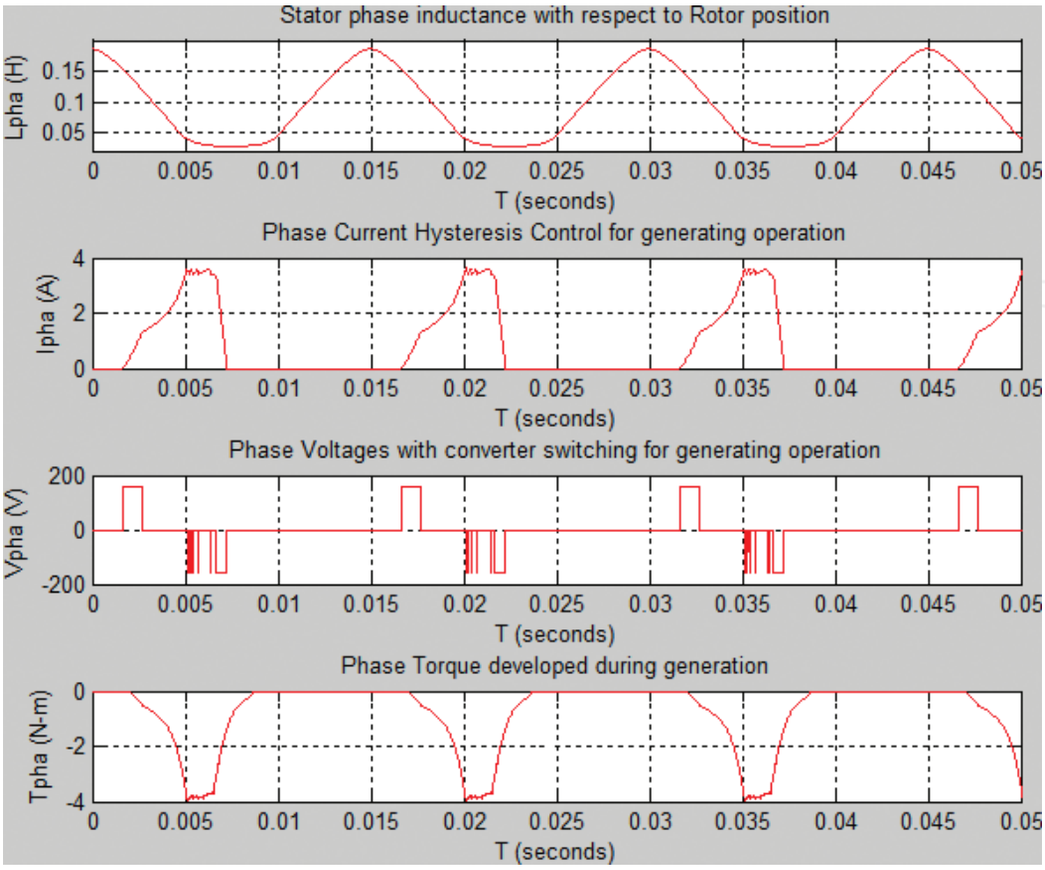

Figure 13. Generating operation of the SRM in forward direction.

d. Single-pulse mode operation: When the machine is operated above the based speed, it is forced to be in the single-pulse mode. In this mode, the phase winding is initially excited with both the switches turned on ($+V_{dc}$) and then demagnetized with both the switches turned off ($-V_{dc}$). Here, the current cannot reach the desired level and decreases to zero when approaching phase commutation point.

8. Conclusion

A Switched Reluctance Machine is special DC machine with non-linear characteristics. This chapter provides modeling approach of two different techniques, one based on the analytical equation and other based on finite element analysis. The techniques provide guidance on how to obtain the optimized commutation angles from the modeling and by utilizing them in the software simulation, the closed-loop control of the SRM in motoring and generating operation are demonstrated. With the optimized commutation angles, precise control of speed, torque, and current in various operational modes in four-quadrants like forward motoring, reverse motoring, forward generation and reverse generation are shown.

Acknowledgements

I wish to express my deep sense of gratitude and indebtedness to my academic advisors, Dr. Yilmaz Sozer and Dr. Iqbal Husain, for their great support in the course of research and opportunity to broaden my horizons.

Author details

Sandeep Narla

Address all correspondence to: narlasandeep@gmail.com

The University of Akron (Alumni), Akron, Ohio, USA

References

[1] Miller TJE. Switched reluctance motors and their control. New York: Magna Physics Publishing and Clarendon Press, Oxford; 1993

[2] Magsoft Corporation. Finite element analysis software reference manual. Troy, New York: Magsoft Corporation; 2010

[3] Radun AV. Design considerations for the switched reluctance motor. IEEE Transactions on Industry Applications. 1995;**31**(5):1079–1087

[4] Dawson GE, Eastham AR, Mizia J. Switched reluctance motor torque characteristics: Finite element analysis and test results. IEEE Transactions on Industrial Applications. 1987;**30**(3):532–537

[5] Husain I, Hossain S. Modeling, simulation and control of switched reluctance motor drives. IEEE Transactions on Industrial Electronics. 2005;**52**(6):1625–1634

[6] Hossain S, Husain I, Klode H, Kequesne B, Omekanda A. Four-quadrant control of a switched reluctance motor for a highly dynamic actuator load. Applied Power Electronics Conference and Exposition, APEC. 7th Annual IEEE, Vol 1. 2002

[7] Hossain S, Husain I. A geometry based simplified analytical model of switched reluctance machines for real-time controller implementation. IEEE Transactions on Power Electronics. 2003;**18**(6):1384–1389

[8] Radun AV. Generating with the switched reluctance motor. In: Proceedings of the IEEE Applied Power Electronics Conference; Dayton, OH, USA; 1994. pp. 41–47

[9] Krishnan R. Switched reluctance motor drive: Modeling, simulation, analysis, design and application. USA: Magna Physics Publishing; 2001

[10] Koibuchi K, Ohno T, Sawa K. A basic study for optimal design of switched reluctance motor by finite element method. IEEE Transactions on Magnetics. 1997;**33**(2):2077–2080

[11] Radun AV. Analytical calculation of the switched reluctance motor's unaligned inductance. IEEE Transactions on Magnetics. 1999;**35**(6):4473–4481

[12] Moallem M, Ong CM. Predicting the torque of a switched reluctance machine from its finite element field solution. IEEE Transactions on Energy Conversion. 1990;**5**(4):733–739

[13] Radun AV. Analytically computing the flux linked by a switched reluctance motor phase when the stator and rotor poles overlap. IEEE Transactions on Magnetics. 2000;**36** (4):1996–2003

[14] Torrey DA. Switched reluctance generators and their control. IEEE Transactions on Industrial Electronics. 2002;**49**:3–14

IntechOpen